The American Journal of Pathology, Vol. 170, No. 4, April 2007

DOI: 10.2353/ajpath.2007.060882

Cardiovascular, Pulmonary and Renal Pathology

Rosuvastatin Treatment Prevents Progressive Kidney Inflammation and Fibrosis in Stroke-Prone Rats

Anita Gianella,* Elena Nobili,* Mauro Abbate,† Carla Zoja,† Paolo Gelosa,* Luciana Mussoni,* Stefano Bellosta,* Monica Canavesi,* Daniela Rottoli,† Uliano Guerrini,* Maura Brioschi,‡ Cristina Banfi,‡ Elena Tremoli,*‡ Giuseppe Remuzzi,† and Luigi Sironi*

From the Department of Pharmacological Sciences, University of Milan, Milan; the Mario Negri Institute for Pharmacological Research,† Bergamo; and the Monzino Cardiologic Center, Istituto di Ricovero e Cura a Carattere Scientifico,‡ Milan, Italy*

Salt-loaded, spontaneously hypertensive stroke-prone rats show progressive increases in blood pressure and proteinuria and accumulate acute-phase proteins in body fluids, modeling events during renal damage. The aim of this study was to assess the pathological events occurring in the kidney of spontaneously hypertensive stroke-prone rats over time and evaluate the effects of statin treatment, which is known to improve renal and cardiovascular outcomes. Kidneys of male spontaneously hypertensive stroke-prone rats euthanized at different stages of proteinuria showed progressive inflammatory cell infiltration, the accumulation of α-smooth muscle actin-positive cells, degenerative changes in podocytes, and severe fibrosis. These were accompanied by an imbalance in the plasminogen/plasmin and metalloprotease systems characterized by the increased renal expression of plasminogen activator inhibitor-1, tissue plasminogen activator, and urokinase plasminogen activator; the net result was an increase in plasmin and matrix metalloproteinase (MMP)-2 and a reduction in MMP-9 activity. Chronic treatment with the hydrophilic rosuvastatin had renoprotective effects in terms of morphology and inflammation and prevented the changes in plasmin, MMP-2, and MMP-9 activity. These effects were independent of the changes in blood pressure and plasma lipid levels. Treatment with the lipophilic simvastatin was not renoprotective. These data suggest that rosuvastatin may have potential utility as a therapeutic option in renal diseases that are characterized by inflammation and fibrosis. ***(Am J Pathol 2007, 170:1165–1177; DOI: 10.2353/ajpath.2007.060882)***

The incidence of chronic renal diseases is increasing worldwide, and there is a great need to identify therapies capable of arresting or reducing disease progression. The current treatment of chronic nephropathies is limited to angiotensin-converting enzyme inhibitors and angiotensin receptor blockers, but there is growing clinical and experimental evidence that statins (3-hydroxy-3-methylglutaryl-CoA reductase inhibitors) could play a therapeutic role.

A post hoc subgroup analysis of the randomized, placebo-controlled Cholesterol and Recurrent Events (CARE) trial in individuals with hyperlipidemia and a history of myocardial infarction demonstrated that pravastatin reduces the rate of declining renal function in patients with moderate to severe renal insufficiency, particularly in those with proteinuria.[1] Another recent post hoc pooled analysis using data from three randomized, double-blind, controlled trials has shown that pravastatin slightly decreases the rate of kidney function loss in patients with or at risk of coronary disease and moderate chronic kidney disease.[2] Furthermore, the results of a prospective study indicate that the combined administration of atorvastatin and an angiotensin-converting enzyme inhibitor or angiotensin receptor antagonist slows the progression of renal disease.[3] Finally, a post hoc analysis of the Treating to New Targets trial data suggests that statin treatment may slow or reverse the decline in renal function normally seen over time in patients with stable coronary disease.[4] Although it is difficult to distinguish the effects that are dependent on, or independent of, their cholesterol-lowering effects in clinical trials, there is emerging evidence that the renoprotection provided by statins is due to their pleiotropic and particularly anti-inflammatory properties. A double-blind, randomized trial investigating the effects of a 6-month treatment on proteinuria in normocholesterolemic patients concluded that pravastatin reduced pro-

A.G. and E.N. contributed equally to this work.

Accepted for publication January 3, 2007.

Address reprint requests to Luigi Sironi, Department of Pharmacological Sciences, University of Milan, Via Balzaretti 9, 20133 Milano, Italy. E-mail: luigi.sironi@unimi.it.

teinuria independently of its lipid-lowering effects by inhibiting the renal synthesis of endothelin-1, a potent proinflammatory agent,[5] and a prospective, randomized trial involving patients with chronic kidney disease found that 20-week treatment with rosuvastatin substantially reduced the levels of the inflammatory biomarker hs-CRP and increased the glomerular filtration rate.[6] A number of *in vivo* studies have found that statins have therapeutic effects on a number of animal models of renal disease in the absence of any changes in lipid levels. Statins interfere with various pathological mechanisms but especially modulate inflammation and fibrotic processes. The renoprotective effects of statins have been reported in animal models of kidney damage resulting from surgery or chemical challenges (ie, ischemia-reperfusion injury, subtotal renal ablation, unilateral ureteral obstruction, or puromycin- or cyclosporine-induced nephropathy).[7–10]

Only few data are available concerning stroke-prone spontaneously hypertensive rats (SHRSPs), a unique model of spontaneously developing hypertension, proteinuria, and histological lesions in the renal vasculature and parenchyma.[11] Renal damage here is not merely the consequence of long-standing hypertension, as closely related spontaneous hypertensive rats develop a similar degree of hypertension but without proteinuria or renal damage. It is known that, in addition to hypertension, the pathogenesis of the renal lesions that invariably precede the appearance of cerebrovascular lesions also includes genetic factors, abnormalities in the renin-angiotensin system, and a high salt intake.

SHRSPs offer an opportunity to disentangle the complex pathological processes occurring during the development of renal failure and to test the effects of potentially renoprotective therapies. We have previously reported that the hydrophilic rosuvastatin, but not the hydrophobic simvastatin, protects against spontaneous brain damage in SHRSPs by modulating local and systemic inflammation without interfering with hypertension or plasma lipid levels.[12] The present study has allowed us to detail for the first time the morphological and cellular alterations occurring in the kidneys of SHRSPs during the salt-loading period and to characterize the mechanisms responsible for the deposition of extracellular matrix. We also investigated the effects of chronic treatment with rosuvastatin and simvastatin to establish whether statins with different physicochemical properties differentially affect the course of the disease and its underlying pathogenetic processes.

Materials and Methods

Animals and Experimental Design

All of the study procedures involving animals and their care were conducted in conformity with the institution's guidelines, which comply with national and international rules and policies. Fifty 6-week-old male SHRSPs (Charles River Laboratories Italia, Calco, Italy) underwent baseline measurements when they were aged 6 weeks. Five were immediately euthanized (time 0) to collect their kidneys, and the other 45 were switched to a permissive low-protein, low-potassium, and high-sodium diet (Japanese permissive diet; Laboratorio Dr. Piccioni, Gessate, Italy: 18.7% protein, 0.63% potassium, and 0.37% sodium) and received 1% NaCl in their drinking water. At the same time, they were randomly divided into three groups for oral treatment by gavage: the animals in group 1 ($n = 15$) served as controls and were treated with 0.5% sodium carboxymethylcellulose (vehicle), those in group 2 ($n = 15$) were treated for 7 weeks with rosuvastatin (supplied by AstraZeneca, London, UK), 10 mg/kg/day dissolved in vehicle, and those in group 3 ($n = 15$) were treated with simvastatin, 10 mg/kg/day dissolved in vehicle. Since the ED_{50} of hepatic cholesterol synthesis is 0.8 mg/kg for rosuvastatin and 1.2 mg/kg for simvastatin, the doses used in this study were comparable.[12] Every week, the rats were weighed, and their systolic arterial blood pressure was measured by means of tail-cuff plethysmography (PB Recorder 8006; Ugo Basile, Comerio, Italy), after which they were housed in individual metabolic cages for 24 hours for the measurement of food and liquid intake and the collection of urine. Blood was drawn every week from the tail vein, and the obtained serum was stored at −20°C until analyzed.

Twenty-four-hour urine protein concentrations were measured according to the Bradford method (Bio-Rad Laboratories, Milan, Italy), using bovine albumin as standard. Five vehicle-treated animals were euthanized when their 24-hour proteinuria exceeded 40 mg/day (time 1). Five rats treated with rosuvastatin and five treated with simvastatin were also euthanized at the same time. A further five control animals were euthanized when their 24-hour proteinuria exceeded 100 mg/day (time 2), and again, at the same time, rats treated with rosuvastatin ($n = 5$) and simvastatin ($n = 5$) were also euthanized. The remaining vehicle-treated rats underwent magnetic resonance imaging[13] every other day until brain damage was observed. At the first appearance of brain abnormalities, they were euthanized (time 3, $n = 5$) with the remaining animals belonging to groups 2 ($n = 5$) and 3 ($n = 5$). The kidneys of all of the animals were collected for histological evaluation, and protein and total RNA was extracted, as described below. The physiological and biochemical parameters were evaluated in all of the available animals at each time point, but the curves in Figure 1 and the lipid values relate to the five animals in each group that survived until time 3.

Proteomic Studies

Urine proteins were concentrated by means of trichloroacetic acid-acetone precipitation. One-dimensional electrophoresis of urine proteins in the presence of sodium dodecyl sulfate (SDS) (without sample reduction) in a discontinuous buffer system on 4 to 20% T-polyacrylamide gradients was performed. The sample load was 3.75 μg per lane.

Renal Histology

Fragments of renal cortex were fixed overnight in Duboscq-Brazil fluid, dehydrated in alcohol, and embedded in par-

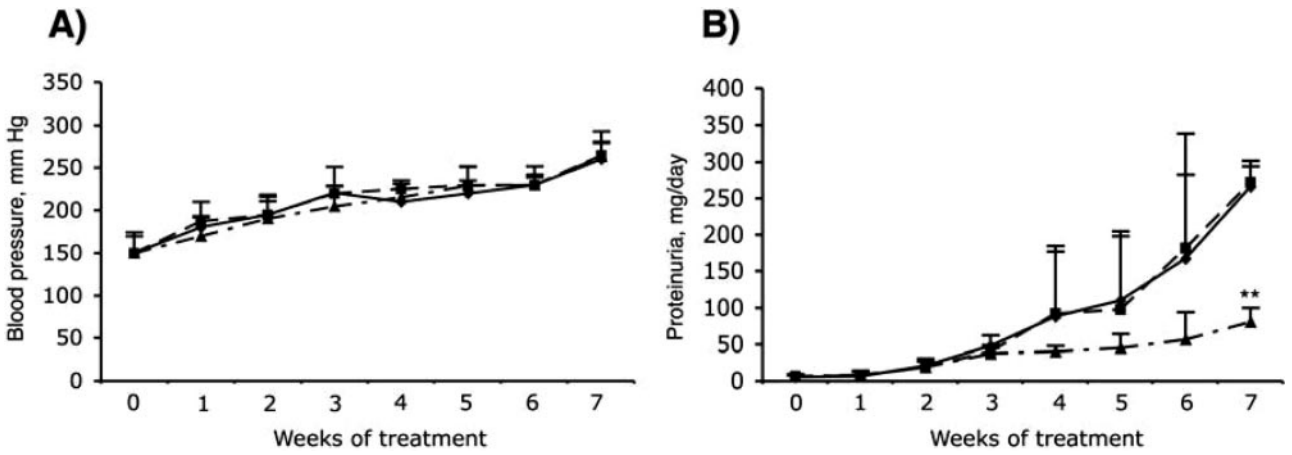

Figure 1. Effect of statins on physiological variables of SHRSPs. Blood pressure (**A**) and daily proteinuria (**B**) as a function of duration of dietary treatment (Japanese permissive diet) in the SHRSPs receiving vehicle (**diamonds**) or treated with 10 mg/kg/day rosuvastatin (**triangles**) or 10 mg/kg/day simvastatin (**squares**). Mean values ± SD, $n = 5$ for each time point and each experimental condition. $^{**}P < 0.01$ versus vehicle- and simvastatin-treated rats.

affin, and 3-μm sections were cut and stained with hematoxylin and eosin, Masson's trichrome, or periodic acid-Schiff reagent. Vascular changes were scored 0 (absent), 1 (mild hyaline deposition and widening of intercellular space in the media), 2 (moderate lesions consisting of arterial and arteriolar hyalinosis and/or hyperplasia), or 3 (severe thickening of the vessel wall). At least 100 glomeruli were examined from each animal, and the extent of glomerular damage was expressed as the percentage of glomeruli with sclerotic lesions. Tubular atrophy and luminal cast formation were assigned separate scores ranging from 0 to 3, respectively, corresponding to absent, mild, moderate and severe changes, and the scores were combined to obtain a mean tubular damage score. All of the renal biopsies were analyzed by the same pathologist, who was unaware of the nature of the experimental groups.

Electron Microscopy

Fragments of kidney tissue were fixed overnight in 2.5% glutaraldehyde in 0.1 mol/L cacodylate buffer (pH 7.4) and washed repeatedly in the same buffer. After postfixation in 1% osmium tetroxide (OsO_4), the specimens were dehydrated through ascending grades of alcohol and embedded in Epon resin. Ultrathin sections were stained with uranyl acetate and lead citrate, and examined using a Philips Morgagni electron microscope (Philips, Brno, Czech Republic). Glomeruli of kidneys taken from three rats randomly selected from the groups given vehicle, rosuvastatin, or simvastatin were first selected on semithin sections. The glomeruli showing sclerotic lesions were not considered for analysis. Four glomeruli were analyzed per animal.

Immunohistochemistry

For the immunohistochemical studies, the kidney specimens in paraffin-embedded slides were dewaxed in xylene and hydrated. Endogenous peroxidase was blocked by adding 1% H_2O_2 in 50% methanol/50% phosphate-buffered saline (PBS), and nonspecific binding sites were saturated with goat serum (DAKO A/S, Glostrup, Denmark). The sections were incubated overnight at 4°C with the primary monoclonal anti-α-smooth muscle actin antibody (1:500; Sigma-Aldrich, St. Louis, MO), rabbit anti-human fibrinogen antibody (1:2000; DAKO A/S), monoclonal antibody against human tissue plasminogen activator (tPA) (1:25; American Diagnostica, Stamford, CT), and rabbit anti-rat plasminogen activator inhibitor-1 (PAI-1) antibody (1:25; American Diagnostica), and then with biotinylated secondary antibodies and streptavidin peroxidase (LSAB2 kit; DakoCytomation).

Horseradish peroxidase was detected using H_2O_2 and diaminobenzidine (Sigma-Aldrich). The extent of the areas immunopositive to α-smooth muscle actin, fibrinogen, tPA, and PAI-1 was measured by means of computer-assisted image analysis (OPTIMAS 6.2; Media Cybernetics, Silver Spring, MD). Microwave-treated paraffin sections were immunohistochemically stained with ED-1 antibody for monocytes/macrophages using a Fast-red technique (Sigma-Aldrich). The number of ED-1-positive cells was counted in at least 20 randomly selected high-power (400×) tubulointerstitial fields.

Sirius Red Staining

Paraffin-embedded kidney tissue sections (5 μm) were dewaxed, hydrated, and stained with Sirius Red F3BA (0.5% in saturated aqueous picric acid) (Sigma-Aldrich), and then examined using polarized light microscopy (Axiovert S100 TV microscope; Zeiss, Jena, Germany) to detect birefringent collagen fibrils. Computer-assisted image analysis (OPTIMAS 6.2; Media Cybernetics) was used to analyze collagen deposition semiquantitatively by measuring the percentage of kidney area positively stained with picrosirius red.

Profile of Renal Plasminogen Activators

The kidney tissue for sodium dodecyl sulfate-polyacrylamide gel electrophoresis (SDS-PAGE) zymography was

weighed, dissected, minced with a scalpel, and extracted using chilled glass homogenizers in ice-cold PBS, 1% Triton X-100, 0.1% SDS, and 0.5% sodium deoxycholate (weight ratio 1:4; PBSTS). The protein concentration was then determined according to Bradford (Bio-Rad Laboratories), and 80-μg extracts were mixed with a nonreducing electrophoresis sample buffer and underwent SDS-PAGE on 11% gel containing 2% casein and 30 μg/ml purified human plasminogen (Hyphen Biomed, Neuville sur Oise, France). To identify uPA, amiloride (2 mmol/L) was added to the SDS-PAGE. Following electrophoresis at 25 mA, the gels were soaked in 2.5% Triton X-100 twice for 30 minutes to remove the SDS and then incubated at 37°C for 3 hours in Tris 0.05 mol/L-NaCl 0.1 mol/L, pH 7.6. The development of lysis bands was revealed by means of 0.1% Coomassie brilliant blue R-250 in 25% methanol and 10% acetic acid. The intensity of each band was quantified using the NIH Image software (Bethesda, MD) and expressed in arbitrary units.

Plasmin Activity

Total renal tissue plasmin activity was measured using a plasmin-specific chromogenic substrate, Chromozym PL (Roche Molecular Biochemicals, Indianapolis, IN), which is specifically cleaved by plasmin into spectrophotometrically detectable 4-nitroaniline and a residual peptide. The renal tissue was suspended at 50 mg/ml in 50 mmol/L Tris, pH 8.2, with 0.1% Triton X-100 and homogenized. After centrifugation at 200 $\times$ *g* for 10 minutes at 4°C, one sample was prepared using 4 μl of the supernatant, 76 μl of 50 mmol/L Tris, pH 8.2, with 0.1% Triton X-100, and 20 μl of 3 mmol/L Chromozym PL with 0.2 μmol/L plasminogen per well in a 96-well plate, and another sample was prepared without plasminogen. The standard linear curve was generated with serial dilutions of bovine plasmin (Roche Molecular Biochemicals). Absorbance was measured at 405 nm every 20 minutes until signal saturation, with increased absorbance corresponding to plasmin activity. The results were expressed as unit per microgram of proteins.

Analysis of Protein Expression for PAI-1

The kidney samples for Western blotting were homogenized in protein extraction buffer [0.025 mol/L ethylene glycol bis(β-aminoethyl ether)-*N*,*N*,*N*′,*N*′-tetraacetic acid, mix-complete 25×, phenylmethylsulfonyl fluoride)] before being centrifuged at 13,000 rpm at 4°C for 20 minutes. The supernatant was collected, and its protein concentrations were determined using the Bradford protein assay. The protein samples (120 μg) were separated by means of 10% SDS-PAGE under reducing conditions and transferred to a nitrocellulose membrane. Immunoblotting for PAI-1 was performed using a commercially available primary rabbit anti-rat PAI-1 antibody (1:500; American Diagnostica). The intensity of the bands corresponding to PAI-1 was normalized using the corresponding β-actin signal as a standard, quantified using the NIH Image software, and expressed in arbitrary units (a.u.).

Matrix Metalloproteinase (MMP) Activity in Kidney Homogenates

MMP activity in tissue homogenates was analyzed by means of gelatin zymography as previously described.[14] The zymograms were quantified by means of densitometric scanning using a digital camera and measured using OPTIMAS 6.2. The results were normalized by cell protein content and expressed as arbitrary optical density units.

Biochemical Analyses

Serum creatinine was measured conventionally and total serum cholesterol, high-density lipoprotein cholesterol, and triglycerides were quantified by means of a commercially available enzymatic reaction kit (ABX, Shefford, UK).

Statistical Analysis

The between-group differences were computed using analysis of variance for repeated measurements, followed by Bonferroni's post hoc test. The densitometry data were analyzed using a two-tailed Student's test and analysis of variance followed by Tukey's test. The renal histology data were analyzed using the nonparametric Kruskal-Wallis test for multiple comparisons. The data are expressed as mean values $\pm$ SD, and a P value of <0.05 was considered significant.

Results

Physiological Effects of Statins

At baseline, the SHRSPs had a systolic blood pressure of 150 $\pm$ 20 mm Hg. Blood pressure in the vehicle-treated rats increased during the Japanese permissive diet and was not influenced by the treatments with rosuvastatin or simvastatin (Figure 1A). The drugs had no effects on food or fluid intake, and body weight increased similarly in the vehicle-, rosuvastatin- and simvastatin-treated rats to 234 $\pm$ 20, 240 $\pm$ 12, and 230 $\pm$ 25 g, respectively, at time 3. Plasma total cholesterol, high-density lipoprotein cholesterol, and triglyceride levels were 44 $\pm$ 4, 23.7 $\pm$ 2.2, and 68 $\pm$ 20, respectively, at baseline (n = 5 for each condition and time; values are in mg/dl); these values did not change significantly during the treatment period in any of the experimental groups (data not shown).

Rosuvastatin but Not Simvastatin Reduces Proteinuria in SHRSPs

After 6 weeks of salt loading, there was a progressive increase in urinary protein excretion, which reached an

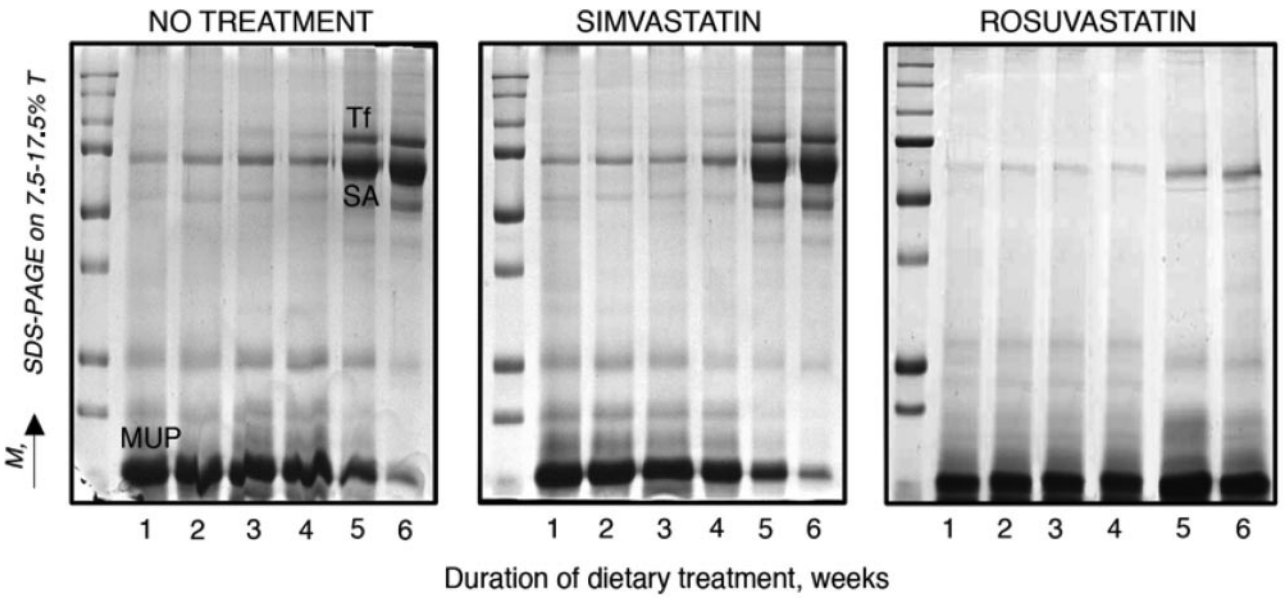

Figure 2. Effect of statins on SHRSPs urinary proteins. Representative one-dimensional electrophoresis of urinary proteins collected weekly from SHRSPs receiving vehicle, 10 mg/kg/day rosuvastatin, or 10 mg/kg/day simvastatin. Samples (3.75 μg) from 24-hour collections in metabolic cages were loaded per lane. The gels are representative of the results obtained in four rats. MUP, major urinary protein; Tf, tranferrin; SA, serum albumin.

average of 266 ± 35 mg/day by 7 weeks in the vehicle-treated SHRSPs and 272 ± 22 mg/day in the animals treated with simvastatin, whereas the rosuvastatin-treated rats showed substantially lower average levels of proteinuria of 80 ± 20 mg/day ($P < 0.01$ versus vehicle and $P < 0.01$ versus simvastatin) (Figure 1B). Qualitative analysis of the excreted proteins by one-dimensional electrophoresis showed that high molecular-weight proteins, previously identified as acute-phase proteins,[15] accumulated dramatically in the urine of the vehicle- and simvastatin-treated rats after 5 to 6 weeks of treatment, whereas rosuvastatin treatment considerably delayed this accumulation (Figure 2).

Renal Function Is Preserved by Rosuvastatin in SHRSPs

Renal function assessed by serum creatinine levels was normal (0.54 ± 0.11 mg/dl) in all of the SHRSP groups at the beginning of the Japanese permissive diet and at times 1 and 2; however, at time 3, the rats given vehicle or simvastatin had high serum creatinine levels (0.96 ± 0.31 and 1.09 ± 0.59 mg/dl, respectively), whereas those treated with rosuvastatin had significantly lower values of 0.56 ± 0.14 mg/dl ($P < 0.05$), comparable with basal serum creatinine levels.

Rosuvastatin but Not Simvastatin Attenuates Renal Lesions and Inflammatory Cell Infiltrates in SHRSPs

The SHRSPs receiving vehicle developed increasingly severe renal lesions over time. Figures 3 and 4 show the effects of the drug treatments on renal lesions and summarize the findings of the semiquantitative analysis. At baseline, the kidneys showed no histological abnormalities (Figure 3A, inset) and, at time 1, when proteinuria averaged 40 to 55 mg/day, showed very mild changes consisting of hyalinosis and edema of the media of the arterial and arteriolar walls (Figure 3A). Similar changes were detected in the rats treated with simvastatin or rosuvastatin at the same time (Figure 3, B and C).

The kidneys of the vehicle-treated rats sampled when proteinuria averaged 100 mg/day (time 2) showed more severe vascular lesions, tubular damage, and glomerular sclerosis in a small percentage of glomeruli (Figure 3D). The structural changes worsened further in the vehicle-treated group of rats showing signs of cerebral edema at the end of the study (time 3), in which sclerosis affected more than 7% of the glomeruli (Figure 3G). The severity and extent of the kidney lesions in the simvastatin-treated rats were comparable with those of the vehicle-treated rats at times 2 and 3 (Figure 3, E and H), whereas the degree of vascular, tubular, and glomerular damage in the kidneys of the rats receiving rosuvastatin was much less severe (Figure 3, F and I). Figure 4 shows the semiquantitative analysis of vascular changes, glomerulosclerosis, and hyaline deposition and tubular changes at the three experimental time points (A, B, and C). After the onset of proteinuria, progressively increasing numbers of ED1+ monocytes/macrophages were found in the interstitium of the rats treated with vehicle (Figures 3J and 4D) or simvastatin (Figures 3K and 4D), but rosuvastatin significantly attenuated the number of interstitial ED1+ cells at all of the time points (Figures 3L and 4D).

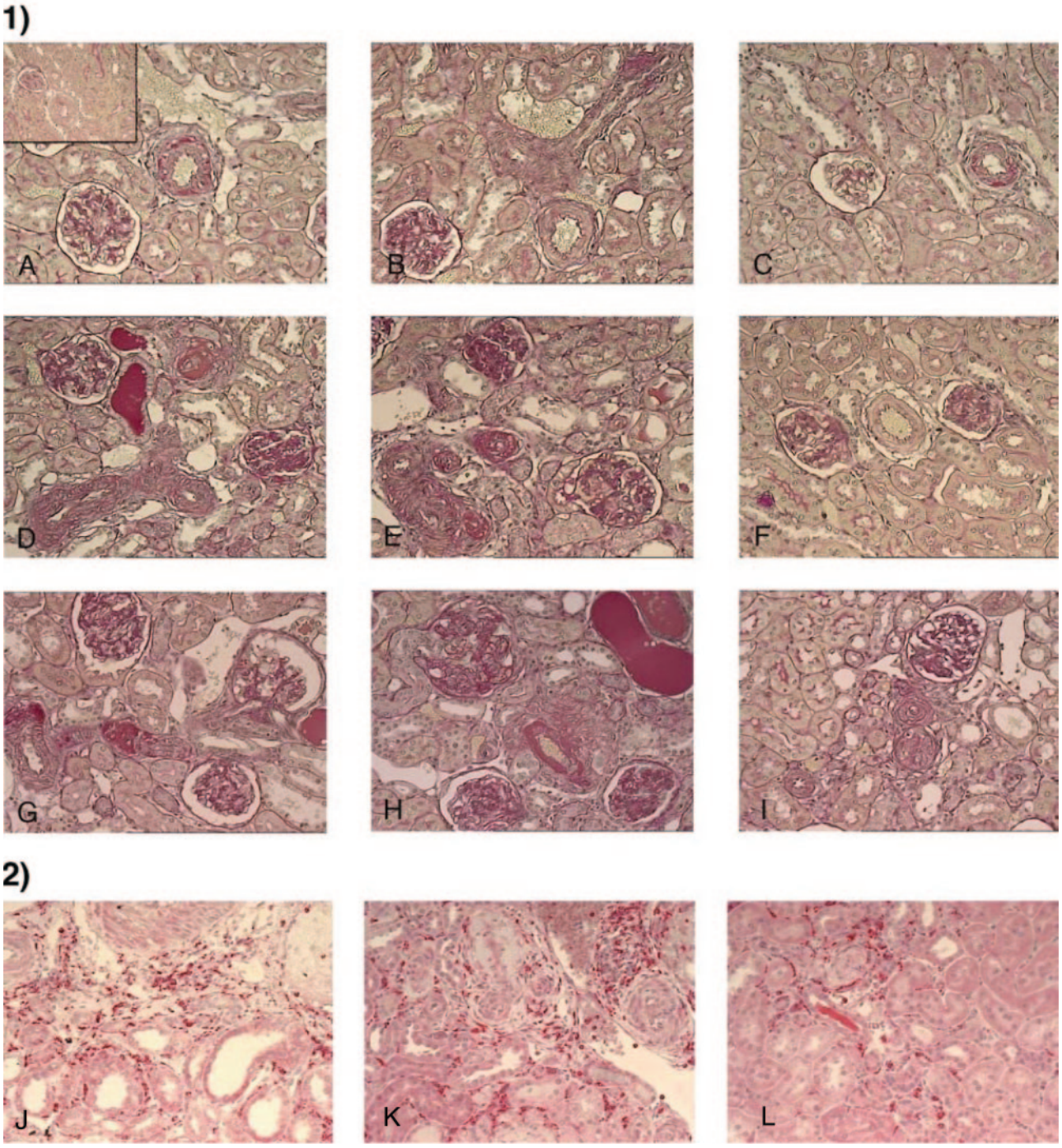

Figure 3. Panel 1: Representative images of histological changes over time in SHRSPs receiving vehicle (**A**, **D**, **G**), simvastatin (**B**, **E**, **H**), or rosuvastatin (**C**, **F**, **I**). In comparison with baseline (**inset** in **A**), there is mild arterial hyalinosis in the vehicle group with early disease (average proteinuria 40 mg/day, **A**); rats with proteinuria averaging 100 mg/day (**D**) or at the end of the study (**G**) show more severe vascular lesions, glomerular sclerosis, and tubular casts. Lesions in rats receiving simvastatin (**B**) or rosuvastatin (**C**) for a short period (time 1) are comparable with those in the vehicle group, but, unlike simvastatin (**E**, **H**), rosuvastatin attenuated renal damage at subsequent time points (**F**, **I**). Periodic acid-Schiff staining, ×150 (**inset**, ×50). **Panel 2:** Immunohistochemical staining of ED-1+ monocytes/macrophages in rats receiving vehicle (**J**), simvastatin (**K**), or rosuvastatin (**L**), and euthanized at time 3. Each panel is representative of results from five rats.

Rosuvastatin Prevents Podocyte Injury in Glomeruli of SHRSP Rats

Electron microscopy showed focal effacement of the foot processes or villous transformation of podocytes in the glomeruli of the SHRSPs given vehicle or simvastatin and euthanized when their proteinuria was still low (time 1) or in a more advanced stage (time 2); the ultrastructural abnormalities were more prominent in the rats euthanized at time 3. The podocytes showed degenerative changes, including extensive villous transformations, cell shape abnormalities, and, notably, focal detachment of the foot

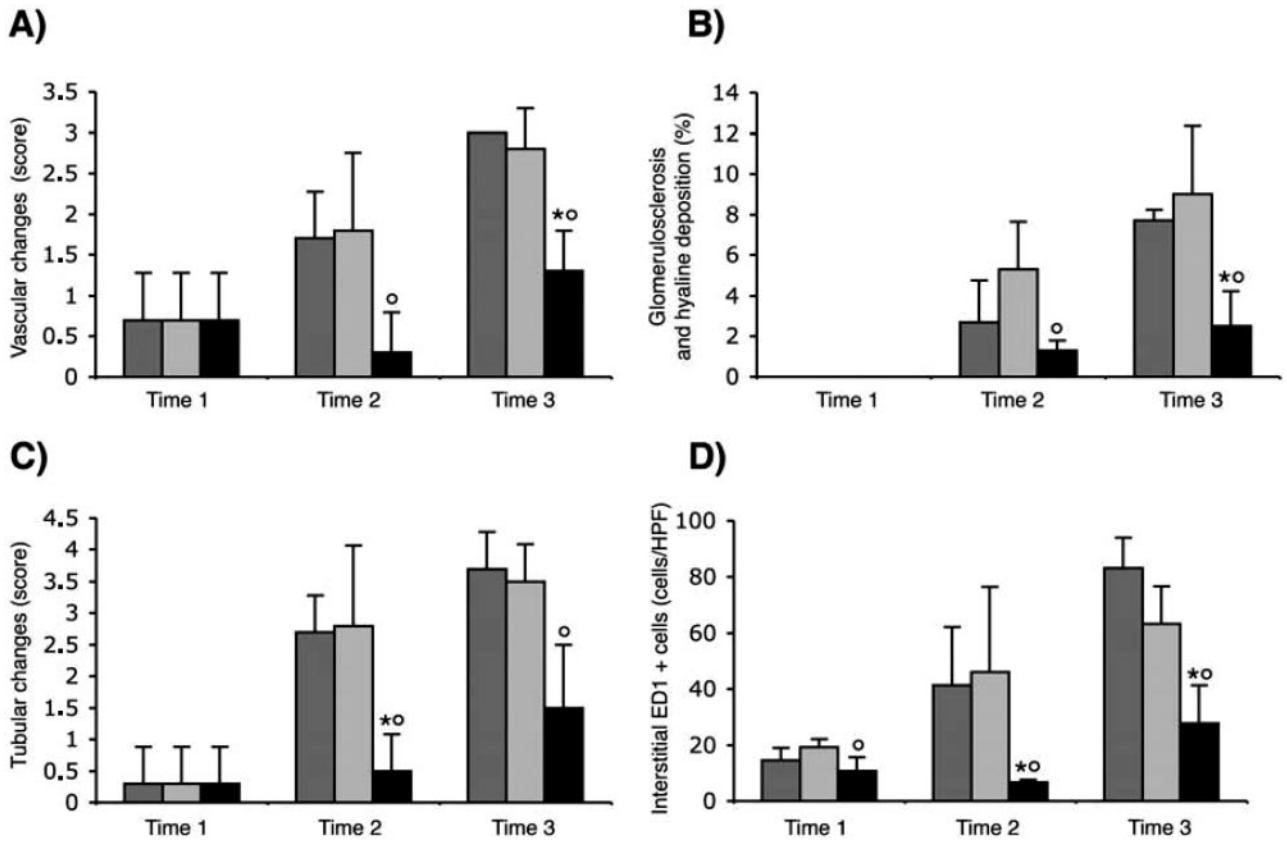

Figure 4. Semiquantitative analysis of vascular (**A**), tubular (**C**), and glomerular histological lesions (**B**), and ED1-positive cell accumulation (**D**), in rats treated with vehicle (dark gray), simvastatin (light gray), or rosuvastatin (black) at the three experimental time points. Mean values ± SD; $n = 5$ for each condition. $^{*}P < 0.05$ versus vehicle-treated rats; $^{\circ}P < 0.05$ versus simvastatin-treated rats at corresponding times. HPF, high-power tubulointerstitial fields.

processes (Figure 5, A and B). The changes in the podocytes of the rats given rosuvastatin (Figure 5C) were much less marked at the end of the study, and focal fusions of the foot processes and microvillous transformations were less frequent. Strikingly, no podocyte detachment was found in the glomeruli of the rosuvastatin-treated rats, which indicates preserved cell interactions with the underlying glomerular basement membrane (Figure 5C).

Effects of Simvastatin and Rosuvastatin on the Kidney Accumulation of α-Smooth Muscle Actin (α-SMA)-Positive Cells, Collagen, and Fibrinogen

Myofibroblasts are considered the main source of the interstitial matrix proteins that accumulate during fibrosis. Staining of the myofibroblast-associated protein α-SMA

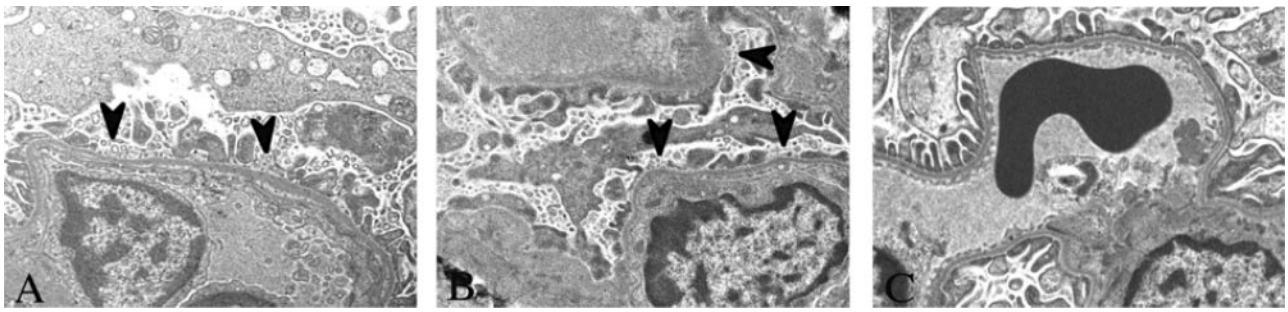

Figure 5. Electron micrographs of glomerular capillary walls in the kidneys of SHRSPs at time 3. Capillary loops in glomeruli of rats given vehicle (**A**) or simvastatin (**B**) show extensive microvillous transformation and focal detachment of podocytes from the glomerular basement membrane (**arrowheads**). **C:** Markedly attenuated ultrastructural changes in a representative glomerulus of a rosuvastatin-treated rat. The results are representative of the data obtained in three different rats for group (×9300).

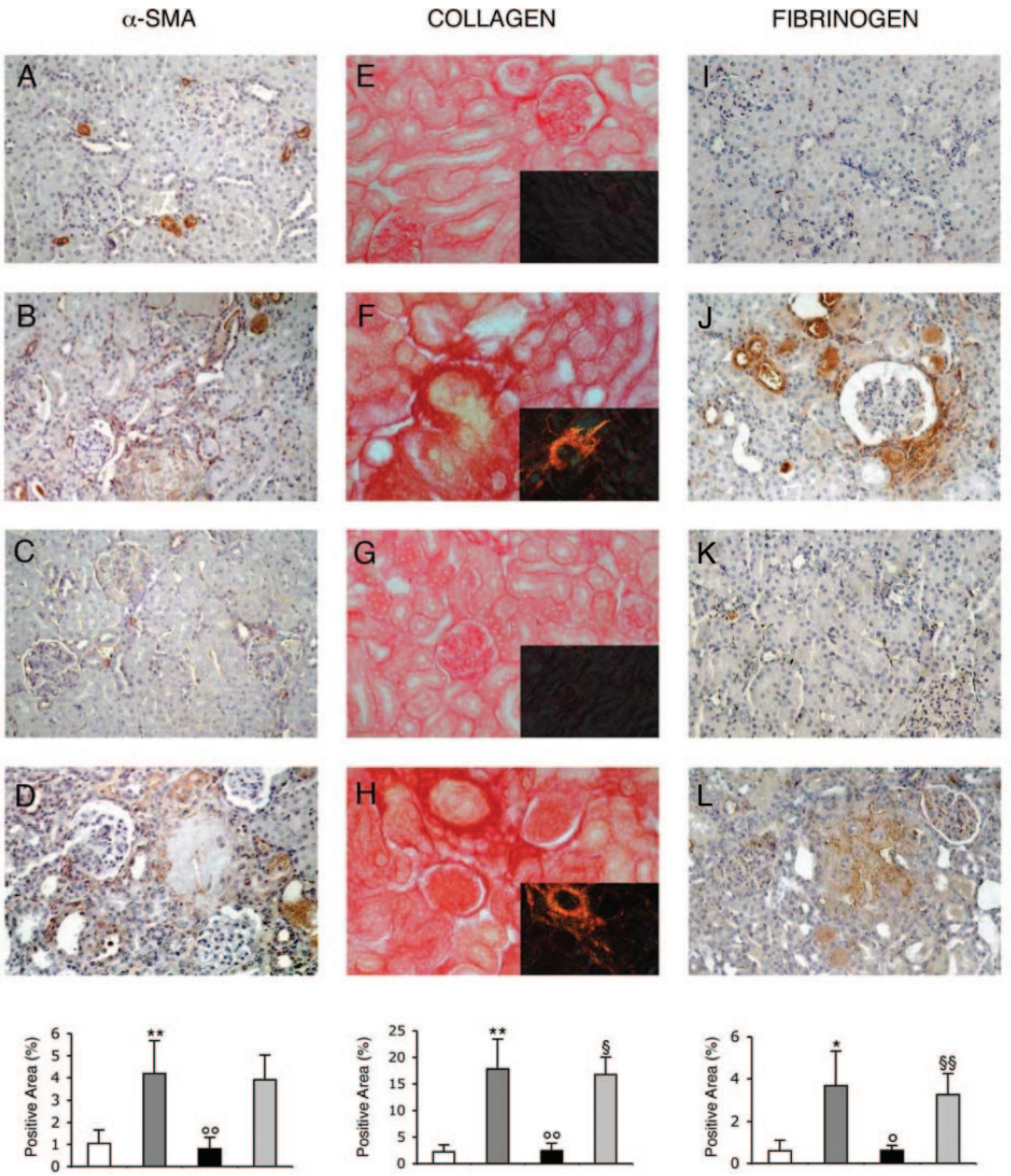

Figure 6. Effects of simvastatin and rosuvastatin on the interstitial accumulation of α-SMA-positive cells and the deposition of interstitial matrix protein. Immunohistochemical staining for α-SMA at baseline (**A**), and in SHRSPs treated with vehicle (**B**), rosuvastatin (**C**), or simvastatin (**D**) at time 3. Representative Sirius red-stained kidney sections at baseline (**E**), and in SHRSPs treated with vehicle (**F**), rosuvastatin (**G**), or simvastatin (**H**) at time 3. The insets show the birefringent collagen fibrils detected using polarized light microscopy. Immunohistochemical staining for fibrinogen at baseline (**I**) and in SHRSPs treated with vehicle (**J**), rosuvastatin (**K**), or simvastatin (**L**) at time 3. Magnification, ×20. Each panel is representative of the results obtained in five rats. The graphs show the extent of the positive areas measured by means of computer-assisted image analysis (OPTIMAS 6.2; Media Cybernetics) expressed as mean values ± SD ($^{*}P < 0.05$ and $^{**}P < 0.01$ versus baseline, $^{\circ}P < 0.05$ and $^{\circ\circ}P < 0.01$ versus vehicle, $^{\S}P < 0.05$ and $^{\S\S}P < 0.01$ versus rosuvastatin) in five kidneys from rats at time 0 (white) and rats treated with vehicle (dark gray), rosuvastatin (black), or simvastatin (light gray).

was significantly higher in the kidneys of the vehicle- or simvastatin-treated rats sampled at time 3 (Figure 6, B and D) than at baseline (Figure 6A), but, as shown in Figure 6C, treatment with rosuvastatin prevented the appearance of abnormal staining for α-SMA in SHRSPs. Evaluated by Sirius red staining, interstitial collagen con-

tent was significantly higher than at baseline in the kidney sections of the animals given vehicle or simvastatin and euthanized at time 3 ($P < 0.01$) (Figure 6, E, F, and H), whereas treatment with rosuvastatin almost completely prevented interstitial collagen deposition (Figure 6G). These data were confirmed using polarized light microscopy to detect birefringent collagen fibrils (Figure 6, E–H, insets). More intense tubular fibrinogen deposits were observed at time 3 in the kidney sections of the vehicle- or simvastatin-treated rats than at baseline (Figure 6, I, J, and L), but rosuvastatin treatment prevented fibrinogen deposition (Figure 6K).

Rosuvastatin Modulates Renal PAI-1 Expression and the Profile of Plasminogen Activator Activity

The effects of rosuvastatin and simvastatin on the system involved in the turnover of matrix deposition were explored at time 3, when the fibrotic processes are exacerbated. Renal PAI-1 protein levels, as measured by Western blotting, were significantly higher at time 3 than at baseline in the vehicle-treated rats euthanized at the end of the study (Figure 7, A and B). Immunostaining particularly revealed tubule PAI-1 expression at this time (Figure 7, C2, D), unlike the minimal or no background staining at baseline (Figure 7, C1, D); rosuvastatin, but not simvastatin, treatment significantly limited PAI-1 protein expression (Figure 7, A and B) and protein staining (Figure 7, C3, C4, D). Baseline plasminogen activators gel zymography of protein extracts showed two distinct lysis bands: one of 40 kd corresponding to uPA and another (barely visible) band of 53 kd corresponding to tPA. No proteolytic activity was detected when the plasminogen was omitted; the 40-kd band disappeared when amiloride (a specific uPA inhibitor) was included in the gel, and the 53-kd band disappeared when a specific antibody against tPA was included (data not shown). As evaluated by the size and intensity of the corresponding bands, in comparison with baseline, tPA and uPA activities increased by 40 and 57%, respectively, in the vehicle-treated rats, and by 31 and 58%, respectively, in the simvastatin-treated rats, but not in those treated with rosuvastatin (Figure 8, A and B). Only tPA-immunostaining experiments could be performed, but they confirmed its accumulation in the renal tubules of the vehicle- and simvastatin-treated rats (Figure 8, C2, C4, D) and the preventive effect of rosuvastatin (Figure 8, C3 and D). No immunostaining was practicable for uPA because of the lack of a suitable antibody.

Plasmin Activity

Total plasmin activity was assessed using the plasmin-specific chromogenic substrate in renal tissue collected at baseline and time 3 from vehicle-, simvastatin-, and rosuvastatin-treated rats. The rats given vehicle or simvastatin showed a considerable increase in plasmin activity at time 3 (respectively 9.66 ± 2.76 and 8.81 ± 2.5 versus 4.11 ± 2.09 U/μg renal protein at baseline; $P < 0.05$ for both vehicle and simvastatin versus baseline);

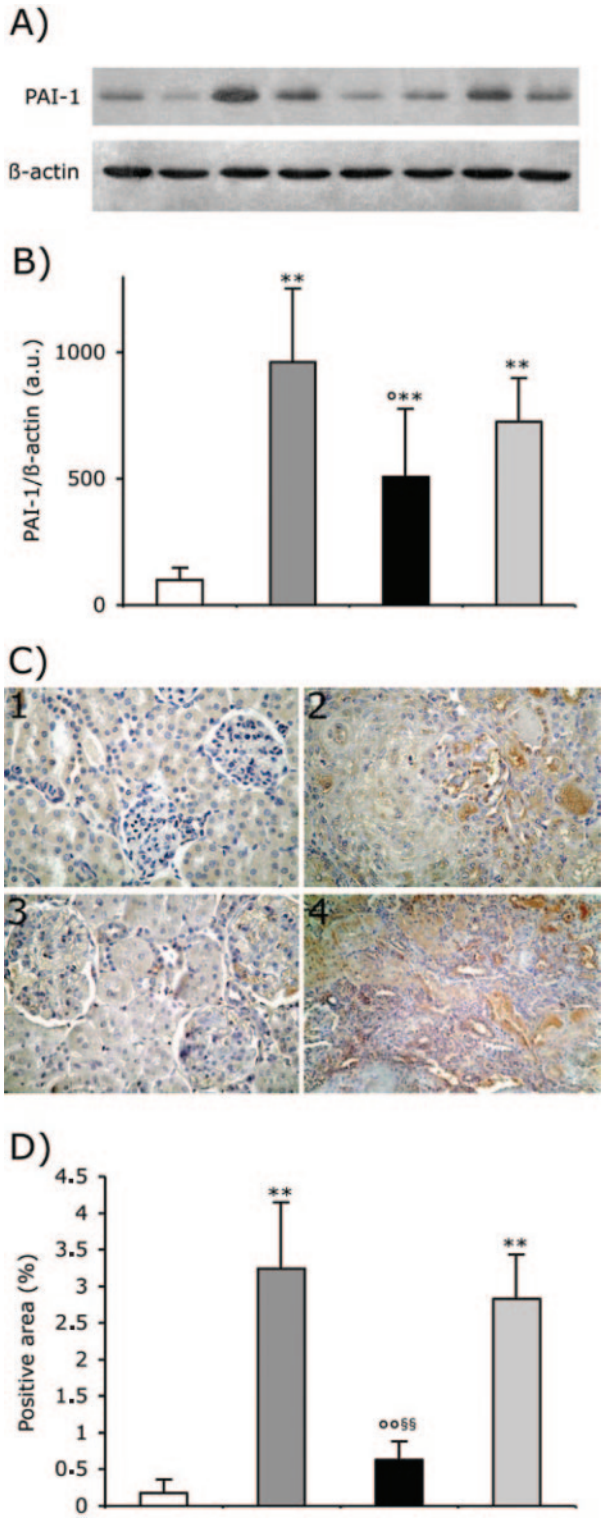

Figure 7. Effect of statins on the renal expression of PAI-1 protein. Western blotting (**A**) of the expression of PAI-1 in the kidney of rats at time 0 (white) and rats treated with vehicle (dark gray), rosuvastatin (black), or simvastatin (light gray) at time 3. The bar graph (**B**) shows the densitometric analysis of the Western blotting normalized to the corresponding β-actin signal; $n = 5$ for each condition. **C:** PAI-1 immunostaining of kidney section at time 0 (**1**) and in rats treated with vehicle (**2**), rosuvastatin (**3**), or simvastatin (**4**) and euthanized when the vehicle-treated rats showed brain damage. The extent of the areas immunopositive to PAI-1 was measured by means of computer-assisted image analysis (OPTIMAS 6.2; Media Cybernetics) (**D**; $n = 5$). $^{**}P < 0.01$ versus baseline; $^{\circ}P < 0.05$ and $^{\circ\circ}P < 0.01$ versus vehicle, $^{\S\S}P < 0.01$ versus simvastatin.

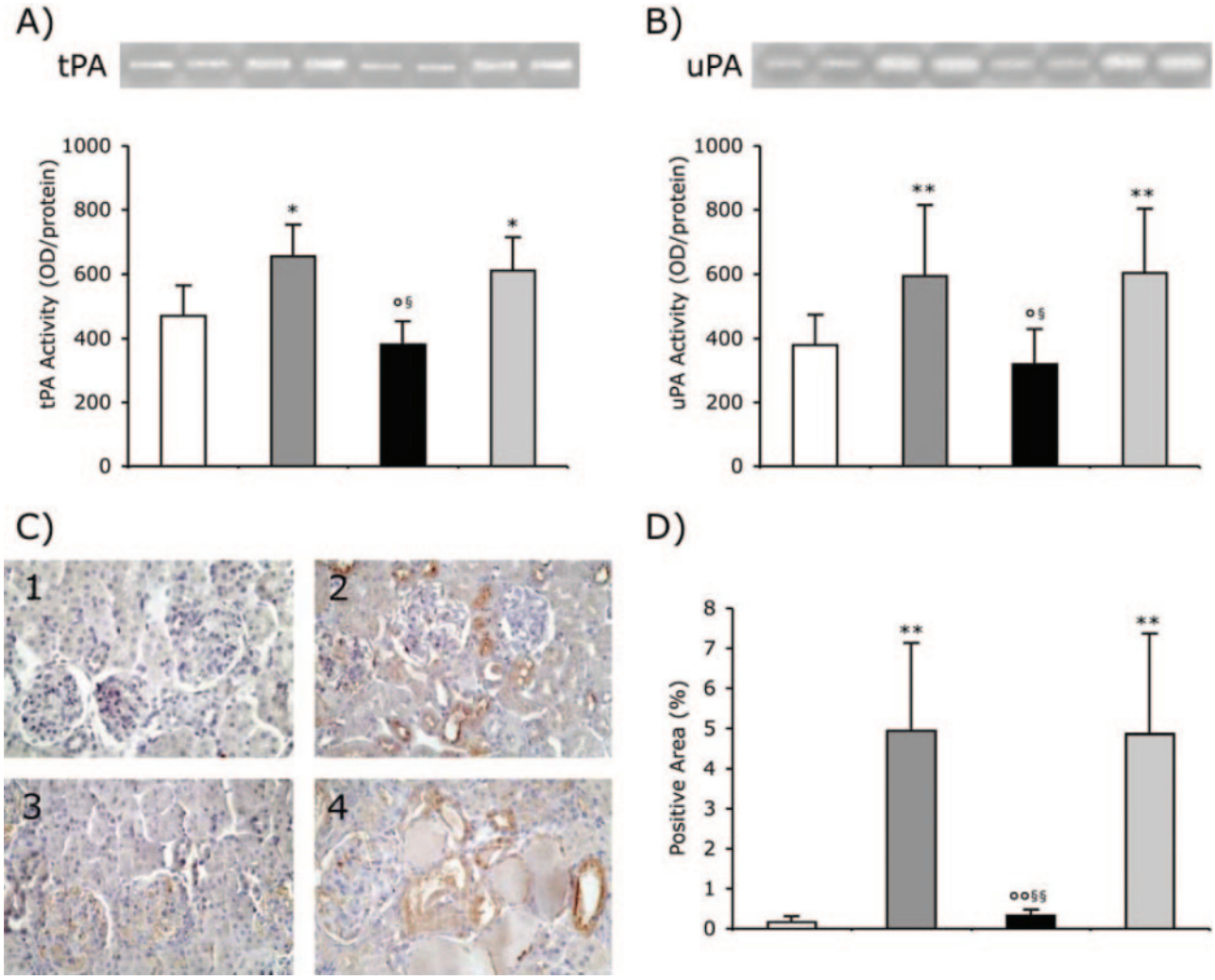

Figure 8. SDS-PAGE zymography of kidney tissue at time 0 (white), and in rats treated with vehicle (dark gray), rosuvastatin (black), or simvastatin (light gray) and sacrificed when the vehicle-treated rats showed brain damage (time 3). **A** shows the upper lysis band of tPA at 53 kd, and **B**, the lower band of uPA at 40 kd. The intensity of each band was quantified using the NIH Image software and expressed in arbitrary units. Data are representative of five individual rats. **C:** tPA immunostaining of kidney section at time 0 (**1**) and in rats treated with vehicle (**2**), rosuvastatin (**3**), or simvastatin (**4**) and euthanized when the vehicle-treated rats showed brain damage. The extent of the areas immunopositive to tPA was measured by means of computer-assisted image analysis (OPTIMAS 6.2; Media Cybernetics) (**D**; $n = 5$). $^{*}P < 0.05$ and $^{**}P < 0.01$ versus baseline, $^{\circ}P < 0.05$ and $^{\circ\circ}P < 0.01$ versus vehicle, $^{\S}P < 0.05$ and $^{\S\S}P < 0.01$ versus simvastatin.

rosuvastatin treatment significantly prevented the increase in renal plasmin activity (5.21 ± 1.44 U/μg renal protein at time 3; $P < 0.05$ versus vehicle and simvastatin).

Rosuvastatin Modulates MMP-2 and MMP-9 Expression

We next evaluated the effect of rosuvastatin and simvastatin treatment on kidney MMP activity. Zymography revealed two proteases with gelatinolytic activity corresponding to MMP-2 and MMP-9 in the renal homogenates collected at time 0. At the time of stroke (time 3), there was a marked and significant decrease in MMP-9-related gelatinolytic activity in the animals receiving vehicle or simvastatin but not in the animals receiving rosuvastatin (Figure 9A). Interestingly, MMP-2 changed in the opposite direction: gelatinase activity was greater at the time of stroke than at baseline in the vehicle- and simvastatin-treated animals, whereas rosuvastatin treatment reduced it (Figure 9B).

Discussion

In this study, we characterized the chain of events occurring in the kidneys of salt-loaded SHRSPs: severe systemic and renal inflammation, severe proteinuria, degenerative changes in podocytes and, in the final stage, massive fibrosis. We also investigated the effects of the lipophilic simvastatin and the hydrophilic rosuvastatin on these pathological events. The results indicate that, although the two statins were administered at doses with comparable pharmacological effects (the ED_{50} of hepatic cholesterol synthesis is 0.8 mg/kg for rosuvastatin and 1.2 mg/kg for simvastatin),[16] their effectiveness in preventing renal damage was markedly different. In particular, without altering plasma lipid levels or blood pres-

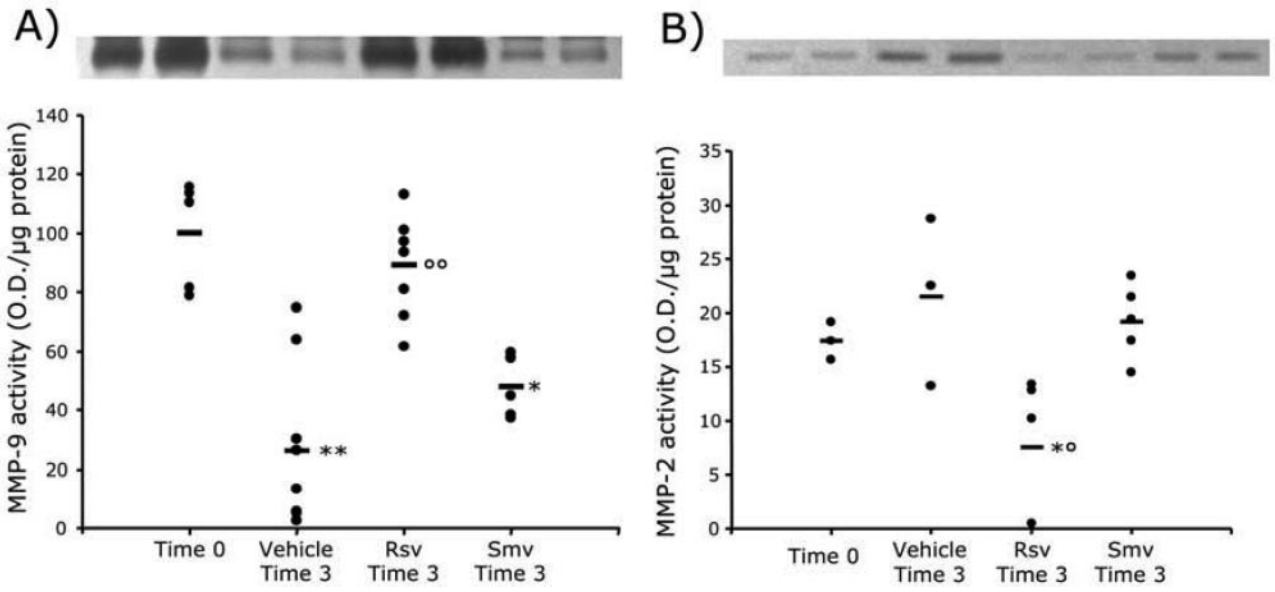

Figure 9. Effect of statins on renal expression of MMP-9 and MMP-2. Gelatinolytic activity and scatter analysis of kidney MMP-9 (**A**) and MMP-2 (**B**) at time 0 and in rats treated with vehicle, rosuvastatin, or simvastatin and euthanized when the vehicle-treated rats showed brain damage (time 3; $n = 5$ each condition). $^{*}P < 0.05$ and $^{**}P < 0.01$ versus time 0; $^{\circ}P < 0.05$ and $^{\circ\circ}P < 0.01$ versus vehicle.

sure, rosuvastatin showed renoprotective effects by preserving renal morphology, reducing inflammatory events, and preventing the increase in plasmin and MMP-2 activity and the decrease in MMP-9 activity, whereas simvastatin had no beneficial effects on any of the evaluated parameters.

These data support previous observations concerning the differences between statins in eliciting nonlipid, or pleiotropic, effects.[17] The mechanisms responsible for these differences have not been investigated in detail but are generically ascribed to pharmacokinetic and pharmacodynamic properties that reflect chemicophysical differences mainly in terms of hydro/lipophilicity. In this respect, the results of *in vivo* and *in vitro* studies have indicated that lipophilic statins are less efficacious in counteracting proinflammatory challenges and, in some cases, may induce or even increase proinflammatory responses at the level of endothelial cells, monocytes and leukocytes.[18,19]

Our data show that rosuvastatin prevented systemic inflammation, as indicated by the decrease in acute-phase urinary proteins, and attenuated local tissue inflammation, such as the accumulation of monocytes/macrophages in the renal interstitium that occurred in both the vehicle- and simvastatin-treated rats. We have previously reported that rosuvastatin abrogates the renal expression of a number of inflammatory mediators in SHRSPs, including interleukin-1β, tumor necrosis factor-α, MCP-1, and transforming growth factor-1β.[12] On the other hand, the renal expression of inflammatory cytokines including MCP-1 and transforming growth factor-1β is enhanced by protein overload of the proximal tubular cells, thus leading to a local accumulation of mononuclear cells and α-SMA-positive cells and the upregulation of matrix protein genes under proteinuric conditions.[20,21] The beneficial effects of rosuvastatin observed in this study were at least partly attributable to significant antiproteinuric action because of the preservation of podocyte integrity (as shown by our ultrastructural findings), and the consequent prevention of the pathogenic effects of a tubular load of ultrafiltered proteins. A rosuvastatin-induced reduction in proteinuria has recently been described in rats with puromycin-induced nephrotic syndrome but not in the rat remnant kidney model.[22,23] Further studies are needed to clarify the reasons underlying such differences and the extent to which rosuvastatin and other hydrophilic statins may have beneficial effects on renal structure in other models of progressive nephropathy.

Salt-loaded SHRSPs show progressive deposition of interstitial matrix proteins. The plasminogen/plasmin and metalloprotease systems are pivotal players in modulating extracellular matrix turnover, and a number of experimental animal models have shown that the two systems influence the progression of renal fibrosis. *In vivo*, statins were shown to reduce renal fibrosis by modulating the plasminogen/plasmin pathway most likely via inhibition of geranylgeranylated Rho protein.[24] The activity of the plasminogen/plasmin system leads to the generation of plasmin from its inactive proenzyme, plasminogen, and plasmin is the result of a complex interaction between the activity of plasminogen activators (tissue-type or urokinase-type plasminogen activators tPA, uPA) and their inhibitor, PAI-1. In our animal model, salt-loading induces an increase in the expression of all the components of the plasminogen/plasmin system and thus leads to increased plasmin activity.

By virtue of its ability to degrade matrix, plasmin could play a protective role in limiting matrix accumulation in renal fibrosis, but it also possesses pathological activity because of leukocyte recruitment[25] and amplification of proteolytic potential because of the activation of MMPs.

Data obtained in mice that are genetically plasminogen-deficient have shown that endogenous plasmin can have deleterious effects on experimentally induced fibrotic injury.[26] Moreover, despite similar renal plasmin activity, mice deficient in PAI-1 or tPA are protected from interstitial fibrosis after ureteral obstruction.[27,28]

It is tempting to speculate that the increased expression of each single component of the plasminogen/plasmin system in our model may have detrimental effects regardless of their actions on plasmin formation. In particular, clinical and experimental studies have shown that PAI-1 is an important mediator of a number of acute and chronic renal diseases,[29] and it has recently been shown that tPA has detrimental effects on renal interstitial fibrogenesis through a cascade of events leading to the destruction of the tubular basement membrane, tubular epithelial-to-myofibroblast transition, and MMP activation.

Conversely, the involvement of uPA in renal diseases is not fully explained, although some experimental evidence indicates it may have protective effects. Under our experimental conditions, salt loading increased both the expression and the activity of tPA and uPA (as evaluated by zymography) as well as the expression of PAI-1 protein. These data are in line with previous findings showing that PAI-1, tPA, and uPA are up-regulated during unilateral ureteral obstruction, a pathological condition characterized by intense fibrosis.[30] The mechanisms underlying these concomitant changes are not known, but PAI-1 expression can be induced by a variety of factors, such as angiotensin II, which is up-regulated by salt loading in SHRSPs, shear stress, hypertension, and cytokines, and it is possible that increased tissue PAI-1 leads to the up-regulation of tPA and uPA.

In addition to the plasminogen/plasmin system, the MMPs (particularly MMP-2 and MMP-9) play a pivotal role in the turnover of extracellular matrix. In our model, salt loading significantly decreased the activity of MMP-9 but had the opposite effect on MMP-2. These findings support previous observations indicating that MMP-9 contributes to the maintenance of the normal structure of the kidney by regulating extracellular matrix turnover. In comparison with their wild-type counterparts, mice that are deficient in MMP-9 develop a more severe form of glomerulonephritis, characterized by proteinuria and massive fibrin deposition, which unequivocally indicates that MMP-9 has protective effects against the development of fibrin-induced renal lesions.[31] MMP-2 acts directly on mesangial cells and induces the development of an inflammatory phenotype,[32] and increased MMP-2 expression has detrimental effects in an animal model of glomerulonephritis.[33] Rosuvastatin treatment establishes a "protective" phenotype by reducing the activity of MMP-2 and increasing that of MMP-9.

In conclusion, SHRSPs develop proteinuria and progressive injury during salt loading as impairment of the plasminogen/plasmin and MMPs systems contribute to the excessive deposition of extracellular matrix. Treatment with the hydrophilic statin rosuvastatin significantly attenuates the severity of the disease. Our findings offer insights into the mechanisms that lead to the fibrotic renal disease occurring in salt-loaded SHRSPs and also indicate that some statins with hydrophilic properties may have the advantage of preventing/reducing the pathological course of renal diseases.

Acknowledgments

We thank Dr. Dario Cattaneo for helpful discussion, and we thank Loredana Bonacina and Andrea Mangolini for their animal husbandry skills.

References

1. Tonelli M, Moye L, Sacks FM, Cole T, Curhan GC: Effect of pravastatin on loss of renal function in people with moderate chronic renal insufficiency and cardiovascular disease. J Am Soc Nephrol 2003, 14:1605–1613
2. Tonelli M, Isles C, Craven T, Tonkin A, Pfeffer MA, Shepherd J, Sacks FM, Furberg C, Cobbe SM, Simes J, West M, Packard C, Curhan GC: Effect of pravastatin on rate of kidney function loss in people with or at risk for coronary disease. Circulation 2005, 112:171–178
3. Bianchi S, Bigazzi R, Caiazza A, Campese VM: A controlled, prospective study of the effects of atorvastatin on proteinuria and progression of kidney disease. Am J Kidney Dis 2003, 41:565–570
4. Shepherd J, Wenger, N, for the TNT Steering Committee and Investigators: Intensive lipid lowering with atorvastatin is associated with a significant improvement in renal function: the Treating to New Targets (TNT) Study. American College of Cardiology 2006 Scientific Sessions, Abstract 2006, 808-3
5. Lee TM, Su SF, Tsai CH: Effect of pravastatin on proteinuria in patients with well-controlled hypertension. Hypertension 2002, 40:67–73
6. Verma A, Ranganna KM, Reddy RS, Verma M, Gordon NF: Effect of rosuvastatin on C-reactive protein and renal function in patients with chronic kidney disease. Am J Cardiol 2005, 96:1290–1292
7. Harris KP, Purkerson ML, Yates J, Klahr S: Lovastatin ameliorates the development of glomerulosclerosis and uremia in experimental nephrotic syndrome. Am J Kidney Dis 1990, 15:16–23
8. Lee SK, Jin SY, Han DC, Hwang SD, Lee HB: Effects of delayed treatment with enalapril and/or lovastatin on the progression of glomerulosclerosis in 5/6 nephrectomized rats. Nephrol Dial Transplant 1993, 8:1338–1343
9. Joyce M, Kelly C, Winter D, Chen G, Leahy A, Bouchier-Hayes D: Pravastatin, a 3-hydroxy-3-methylglutaryl coenzyme A reductase inhibitor, attenuates renal injury in an experimental model of ischemia-reperfusion. J Surg Res 2001, 101:79–84
10. Moriyama T, Kawada N, Nagatoya K, Takeji M, Horio M, Ando A, Imai E, Hori M: Fluvastatin suppresses oxidative stress and fibrosis in the interstitium of mouse kidneys with unilateral ureteral obstruction. Kidney Int 2001, 59:2095–2103
11. Yamashita T, Kawashima S, Miwa Y, Ozaki M, Namiki M, Hirase T, Inoue N, Hirata K, Yokoyama M: A 3-hydroxy-3-methylglutaryl coenzyme A reductase inhibitor reduces hypertensive nephrosclerosis in stroke-prone spontaneously hypertensive rats. J Hypertens 2002, 20:2465–2473
12. Sironi L, Gianazza E, Gelosa P, Guerrini U, Nobili E, Gianella A, Cremonesi B, Paoletti R, Tremoli E: Rosuvastatin, but not simvastatin, provides end-organ protection in stroke-prone rats by antiinflammatory effects. Arterioscler Thromb Vasc Biol 2005, 25:598–603
13. Guerrini U, Sironi L, Tremoli E, Cimino M, Pollo B, Calvio AM, Paoletti R, Asdente M: New insights into brain damage in stroke-prone rats: a nuclear magnetic imaging study. Stroke 2002, 33:825–830
14. Bellosta S, Via D, Canavesi M, Pfister P, Fumagalli R, Paoletti R, Bernini F: HMG-CoA reductase inhibitors reduce MMP-9 secretion by macrophages. Arterioscler Thromb Vasc Biol 1998, 18:1671–1678
15. Sironi L, Tremoli E, Miller I, Guerrini U, Calvio AM, Eberini I, Gemeiner M, Asdente M, Paoletti R, Gianazza E: Acute-phase proteins before cerebral ischemia in stroke-prone rats. Stroke 2001, 32:753–760
16. McTaggart F, Buckett L, Davidson R, Holdgate G, McCormick A, Schneck D, Smith G, Warwick M: Preclinical and clinical pharmacology of rosuvastatin, a new 3-hydroxy-3-methylglutaryl coenzyme A reductase inhibitor. Am J Cardiol 2001, 87: 28B–32B

17. Chong PH, Seeger JD, Franklin C: Clinically relevant differences between the statins: implications for therapeutic selection. Am J Med 2001, 111:390–400
18. Kiener PA, Davis PM, Murray JL, Youssef S, Rankin BM, Kowala M: Stimulation of inflammatory responses in vitro and in vivo by lipophilic HMG-CoA reductase inhibitors. Int Immunopharmacol 2001, 1:105–118
19. Matsumoto M, Einhaus D, Gold ES, Aderem A: Simvastatin augments lipopolysaccharide-induced proinflammatory responses in macrophages by differential regulation of the c-Fos and c-Jun transcription factors. J Immunol 2004, 172:7377–7384
20. Zoja C, Benigni A, Remuzzi G: Cellular responses to protein overload: key event in renal disease progression. Curr Opin Nephrol Hypertens 2004, 13:31–37
21. Abbate M, Zoja C, Rottoli D, Corna D, Tomasoni S, Remuzzi G: Proximal tubular cells promote fibrogenesis by TGF-beta1-mediated induction of peritubular myofibroblasts. Kidney Int 2002, 61:2066–2077
22. Liang K, Kim CH, Vaziri ND: HMG-CoA reductase inhibition reverses LCAT and LDL receptor deficiencies and improves HDL in rats with chronic renal failure. Am J Physiol Renal Physiol 2005, 288:F539–F544
23. Vaziri ND, Liang K: Effects of HMG-CoA reductase inhibition on hepatic expression of key cholesterol-regulatory enzymes and receptors in nephrotic syndrome. Am J Nephrol 2004, 24:606–613
24. Essig M, Vrtovsnik F, Nguyen G, Sraer JD, Friedlander G: Lovastatin modulates in vivo and in vitro the plasminogen activator/plasmin system of rat proximal tubular cells: role of geranylgeranylation and Rho proteins. J Am Soc Nephrol 1998, 9:1377–1388
25. Ploplis VA, French EL, Carmeliet P, Collen D, Plow EF: Plasminogen deficiency differentially affects recruitment of inflammatory cell populations in mice. Blood 1998, 91:2005–2009
26. Edgtton KL, Gow RM, Kelly DJ, Carmeliet P, Kitching AR: Plasmin is not protective in experimental renal interstitial fibrosis. Kidney Int 2004, 66:68–76
27. Oda T, Jung YO, Kim HS, Cai X, Lopez-Guisa JM, Ikeda Y, Eddy AA: PAI-1 deficiency attenuates the fibrogenic response to ureteral obstruction. Kidney Int 2001, 60:587–596
28. Yang J, Shultz RW, Mars WM, Wegner RE, Li Y, Dai C, Nejak K, Liu Y: Disruption of tissue-type plasminogen activator gene in mice reduces renal interstitial fibrosis in obstructive nephropathy. J Clin Invest 2002, 110:1525–1538
29. Eddy AA: Plasminogen activator inhibitor-1 and the kidney. Am J Physiol Renal Physiol 2002, 283:F209–F220
30. Ishidoya S, Ogata Y, Fukuzaki A, Kaneto H, Takeda A, Orikasa S: Plasminogen activator inhibitor-1 and tissue-type plasminogen activator are up-regulated during unilateral ureteral obstruction in adult rats. J Urol 2002, 167:1503–1507
31. Lelongt B, Bengatta S, Delauche M, Lund LR, Werb Z, Ronco PM: Matrix metalloproteinase 9 protects mice from anti-glomerular basement membrane nephritis through its fibrinolytic activity. J Exp Med 2001, 193:793–802
32. Turck J, Pollock AS, Lee LK, Marti HP, Lovett DH: Matrix metalloproteinase 2 (gelatinase A) regulates glomerular mesangial cell proliferation and differentiation. J Biol Chem 1996, 271:15074–15083
33. Kuroda T, Yoshida Y, Kamiie J, Kovalenko P, Nameta M, Fujinaka H, Yaoita E, Endo T, Ishizuka S, Nakabayashi K, Yamada A, Nagasawa T, Yamamoto T: Expression of MMP-9 in mesangial cells and its changes in anti-GBM glomerulonephritis in WKY rats. Clin Exp Nephrol 2004, 8:206–215